Water droplet motion under the influence of Surface Acoustic Waves (SAW)

Journal of Physics Communications

PAPER

Water droplet motion under the influence of Surface Acoustic Waves (SAW)

Zinetula Insepov[1,2,3], **Zamart Ramazanova**[1], **Nurkhat Zhakiyev**[1,4] and **Kurbangali Tynyshtykbayev**[1]

[1] Nazarbayev University, 010000, 53 Kabanbay Batyr Ave, Nur-Sultan, Kazakhstan
[2] Purdue University, 500 Central Drive, West Lafayette, IN IN 47907, United States of America
[3] National Research Nuclear University (MEPhI), 31 Kashira Hwy, Moscow, 115409, Russia
[4] Astana IT University, 010000, 53 Mangilik Yel Ave, Nur-Sultan, Kazakhstan

E-mail: zinsepov@purdue.edu

Keywords: water actuation, Surface Acoustic Waves, SAW device, droplet motion, streaming

OPEN ACCESS

RECEIVED
10 June 2020

REVISED
6 January 2021

ACCEPTED FOR PUBLICATION
8 January 2021

PUBLISHED
17 March 2021

Abstract

The water droplet motion processes actuated by applying surface acoustic waves at various RF powers and frequencies were investigated by numerically modelling and compared with experiment. A three-dimensional computational model of a free water droplet streaming on the surface of the substrate have been developed using Finite Element Method (FEM) with Laminar Two-Phase Flow Moving Mesh approach for Navier–Stokes equations which were coupled with Convection Wave equation (CWE) module of the COMSOL Multiphysics. Water droplet motion speeds were experimentally measured and confirmed for water droplets with the volumes of 2 and 5 μl, at SAW frequencies 34 and 58 MHz, and power range 0.1–1.23 W. The effect of frequency on microfluidic performance such as streaming flows and droplet motion has been studied both numerically and experimentally toward developing MEMS devices for future energy sources, e.g., for direct methanol fuel cells, hydrogen energy, as well as for use in a wide variety of chemical, water desalination and purification of other fluids from salts, germs, bacteria, and viruses based on perspective multiphysical effects.

1. Introduction

Recently, there has been an increased interest in surface acoustic waves (SAW)-based micro devices for different applications based on a mix of the multiphysical effects using new features of perspective materials. Nanopumping effects [1, 2] can be used for the development of a new energy-saving methods of purification and desalination of water. Existing micro- and sub-micro-sized filters for water purification are generally unsuitable for restoring them after the expiration date due to contamination, since filter cleaning from clogging is a much more energy-consuming process than creating a submicron membrane. Therefore, this work is crucial for the development of a new method of the delivery in nanomedicine and MEMS. When SAW propagates on a surface of a piezoelectric device and encounters the droplet, the surface energy penetrates into a droplet and generates longitudinal waves at a Rayleigh angle [3]. As a result, the wave energy creates a volume force on the droplet and move in the direction of SAW. Then it generates various internal effects, such as vibrating, pumping, streaming, jetting formation, and atomization of the droplet. A linear relationship on microfluidic performance between the SAW power, frequency and streaming velocity has been obtained and investigated in [4–8]. The main internal flow in the water droplet is viscous and periodic as a resulted sum of forces of the propagating SAW and contact between the liquid and the solid surface. This flow further drifts the liquid mass along the Rayleigh SAW direction and well known as the Schlichting streaming [7].

Alghane *et al* studied the streaming behaviour of a liquid droplet as a function of radio-frequency (RF) power and droplet size [9], and simulated numerically a SAW-driven mixing process of the dye particles inside microdroplets, and verified experimentally, to investigate the effect of SAW excitation frequency in the flow streaming and mixing process for a range of droplet volumes and RF powers [10]. In paper Alvarez *et al* [11] has been characterized the manufacturing of SAW atomizer and shown the ability of atomizer to form

monodisperse aerosols for drug delivery application. Kurosawa *et al* [12, 13] have proposed a novel way to produce dry fog using a surface acoustic wave transducer. An ultrasonic atomizer using SAW at the frequency of 10 MHz was described. In work [14] the atomizer was expected to function as a pump by using the wave-guide. Fu *et al* [15] investigated streaming, micromixing, and micropumping effects by SAW on ZnO film. Du *et al* [16] have provided a detailed studied induced acoustic streaming and pumping, focusing on the effects of the wave mode and surface modification on SAW. Both of the waves have showcased the capability to produce acoustic streaming and to pump liquid.

In the paper Guo *et al* [8] SAW devices on the bases of $LiNbO_3$ and ZnO/Si substrates with various resonant frequencies from 62 MHz to 275 MHz have been fabricated and described, and then the impact of SAW frequency and power on microfluidic characteristics such as streaming, pumping and jetting was investigated. Transportation of microscopic grains by plate acoustic waves purposed and investigated in [17], two- and three-dimensional FEM modeling of droplet dynamics under the influence of gravity force on complex surfaces shown in [18, 19]. Numerical modeling study of a free water droplet moving under influence of SAW was carried out by a FEM using Comsol Multiphysics package [20]. In the paper Liang W. and Lindner G. (2013) the inhomogeneous acoustic streaming force field induced by Lamb waves in the droplet was calculated by solving the surface tension and incompressible Navier–Stokes equations using the moving mesh mode of the COMSOL software [21]. Biroun *et al* (2019) developed a coupled level set volume of fluid approach for investigation transportationa and jetting behaviours of the droplet driven by thin-film SAW. This approach includes two-phase flow and interfacial phenomena such as surface tension, dynamic contact angles and liquid-interactions with SAW [22]. A SAW-based acoustophoretic microdevice in 2D formulation modeled for fluid-filled microchannel resting on a piezoelectric substrate in [23]. A different computational fluid dynamics (CFD) simulation platforms helps model the processes by defining geometry, meshing sample, specifying physics, solving, and then, visualizing the results [24]. The tools can help to quickly cope with complex problems of linear and nonlinear processes, as well as post-processing.

The obtained experimental results were compared with the simulation of water droplet moving under the influence of SAW. COMSOL Multiphysics allows solving multi-physics problems involving combination of various physical problems described by partial differential equations and therefore, provides detailed analysis of a complex physical model.

2. Experiment

Using photolithography, the test's SAW devices were fabricated on the basis of the YZ-cut of a $LiNbO_3$ crystal with an Al interdigital transducer (IDT) structure generating SAW with a wavelength of $\lambda = 60$ μm at the resonance excitation frequency of f = 58 MHz; and an IDT structure emitting SAW with a wavelength of $\lambda = 100$ μm at the resonance excitation frequency of f = 34 MHz. The generated SAW propagates in the *YZ*-cut of the $LiNbO_3$ crystal along the *Z*-axis at the velocity of V = 3488 m s^{-1}. A high-frequency generator APH-2140, with regulated power 0.1–1.23 W, 0–5 dBm, were used for generation of SAW.

Characterization of water liquid droplet motion under the influence of SAW was performed by video recording, using a Sony 720 × 480 video camera at a speed of 25 frames per second.

Figure 1 shows the fragments (a-k) of a liquid droplet moving through membranes under the action of SAW. Figure 1(a) shows the initial droplet, before the high-frequency generator is turned on, and the RF signal was applied to the IDT 1; figure 1(b)—at the moment when HF signal is applied on the IDT 1; figure 1(c)—the droplet reaches the first membrane and begins to leak through it; figure 1(d), the droplet begins to percolate through the membrane, the initial part of the droplet is still visible after the passage of the membrane and the tail part of the droplet is also clearly visible; fragments figures 1(d)–(g)—show the passage of the droplet through the first membrane, and formation of the front part of a large droplet after the passage through membrane, and the decay of the tail part of the droplet into small fragments; figure 1(h)—fragment of reaching the second membrane; figures 1(i)–(k) fragments of the passage of the droplet through the second membrane. It can be seen (figure 1(b)–(h)) that the droplet of liquid in the form of a moving 'caterpillar' passes the first membrane. And after filtering on the first filter, a filtered liquid or finely dispersed droplet slips through the subsequent membranes (see red numbers in figures 1(d)–(k)). Sequential side view images provided in the appendix figure A.1.

In the experiment, the free droplet velocity before reaching membranes (figures 1(a)–(c)) was measured from 0.5 cm s^{-1} to 4.5 cm s^{-1}, depending on the volume of the droplets and the SAW power (figure 2).

The simulation results are important for clarifying the mechanism of interaction of SAW with a water droplet and for designing laboratory devices on chips.

Based on the collected experimental data on nanofiltration of droplet through the membrane actuated by SAW, the analysis of interdependencies between the supplied power (W), volumes of droplets (μl), frequencies

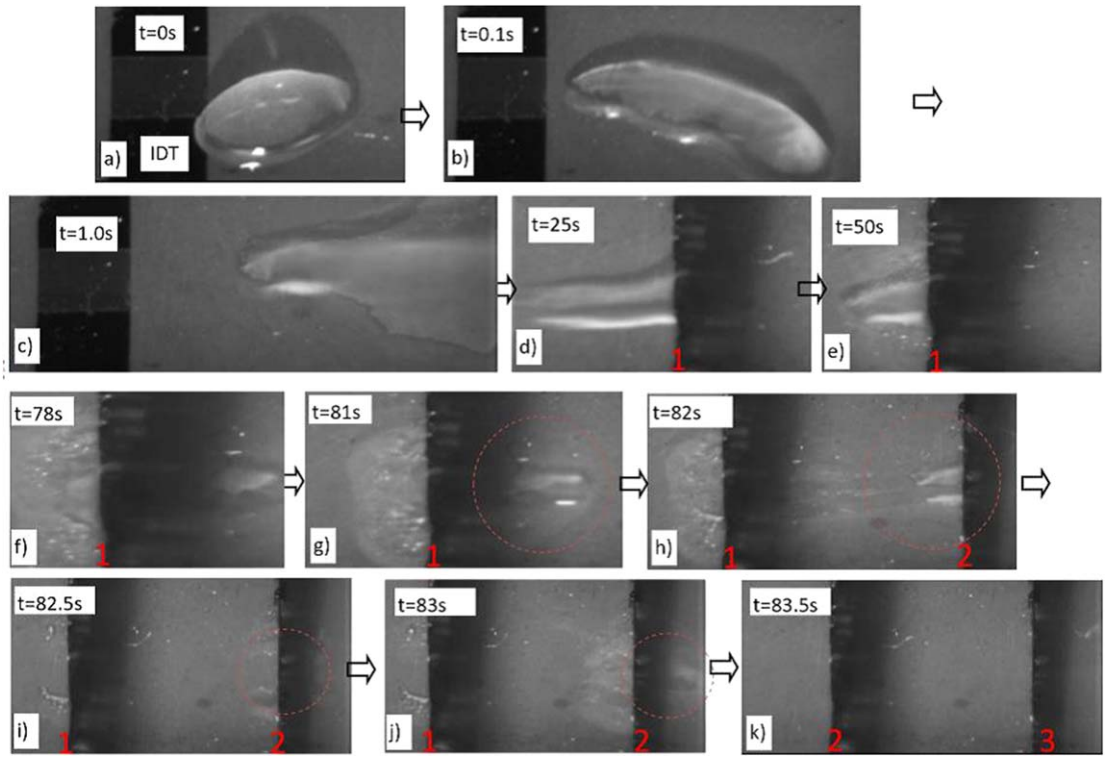

Figure 1. Sequential top view images of the 2 μl droplet filtration dynamics under the influence of SAW through three Nafion membranes, each image has time indicators (letters flow from left to right). Transducer located in the right side, Red numbers are indicated number of membranes.

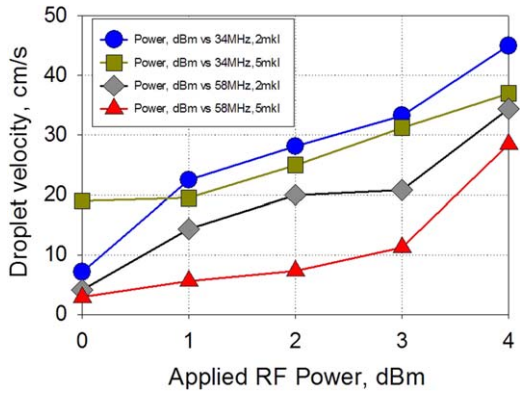

Figure 2. Experimental results for water droplet velocities, mm s^{-1}, for a given applied power, frequencies, and droplet's volumes.

(MHz), types of liquids (water, 50% alcohol solution in water), the speeds of movement of the droplet, and the rate of passage through the filters were obtained.

In this paper, we have experimentally observed the water droplet with various frequencies 34 and 58 MHz and a volume of 2 and 5 μl. Based on the collected experimental data the analysis of interdependencies between the supplied power (W), volumes of droplets (μl), frequencies (MHz), types of liquids (water, 50% alcohol solution in water), and the speeds of movement of the droplet were obtained.

The effect of SAW frequency on microfluidic characteristics, such as streaming, atomization, and passage of a droplet through a membrane studied experimentally using a video camera in the power range of 0.1–1.23 W. The obtained results and the simulation of water movement through nanomembranes will be published elsewhere. Figure 3 shows the video recording of the experimental results for droplets of 2 and 5 μl in volume where the frames were positioned of the scale bar to be able to calculate the speed of the droplet.

The droplet's speed measured using video recording was obtained within the range of 0.5–3.5 cm s^{-1} (figure 2), with an average speed of 2.23 cm s^{-1}, for the experimental applied power.

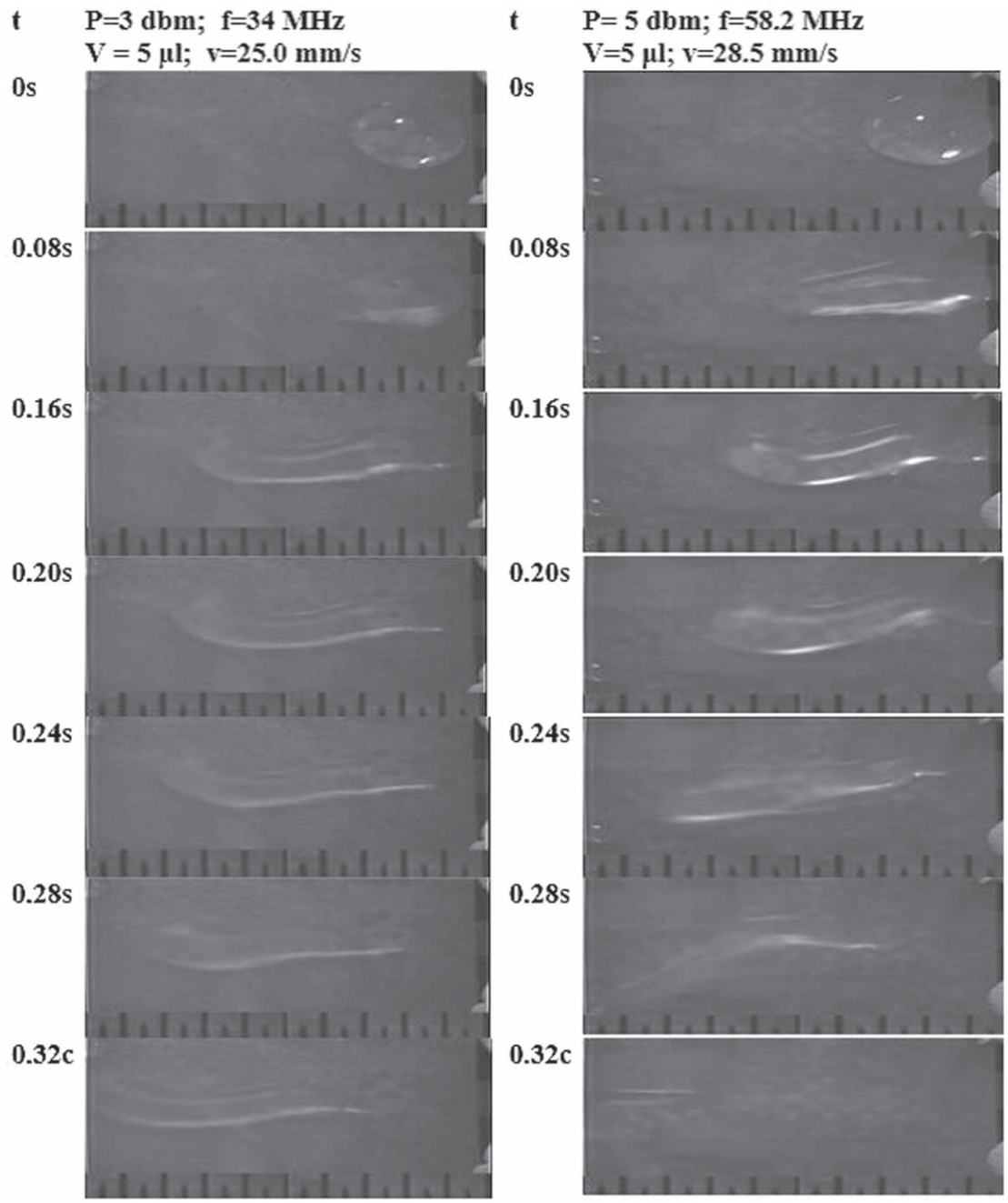

Figure 3. Sequential top view images of the droplet dynamics under the influence of SAW before reaching membranes, each image has time indicators. The transducer located in the right side, direction of the droplet's movement is from right to left. a) a 5 μl water droplet movement under influence of SAW with 34 and 58 MHz; b) a 2 μl water droplet movement under influence of SAW with 3 dBm and 2 dBm power.

3. Simulation

In this paper, we have developed a three-dimensional mathematical model of SAW propagation and SAW actuation of a water droplet on a Lithium Niobate piezoelectric substrate using Comsol Multiphysics [20] with 3D visualisation tools. This model allows us to study SAW and water motion process on the substrate and to calculate fluid flow rate, flow velocity, and RF signal voltage and droplet volume dependences on time.

3.1. Model description

Modeling consisted of two parts. A piezoelectric substrate with interdigital transducers (IDT) was simulated to determine the eigenfrequencies localization of SAW at the solid-liquid interface. Then these frequencies were

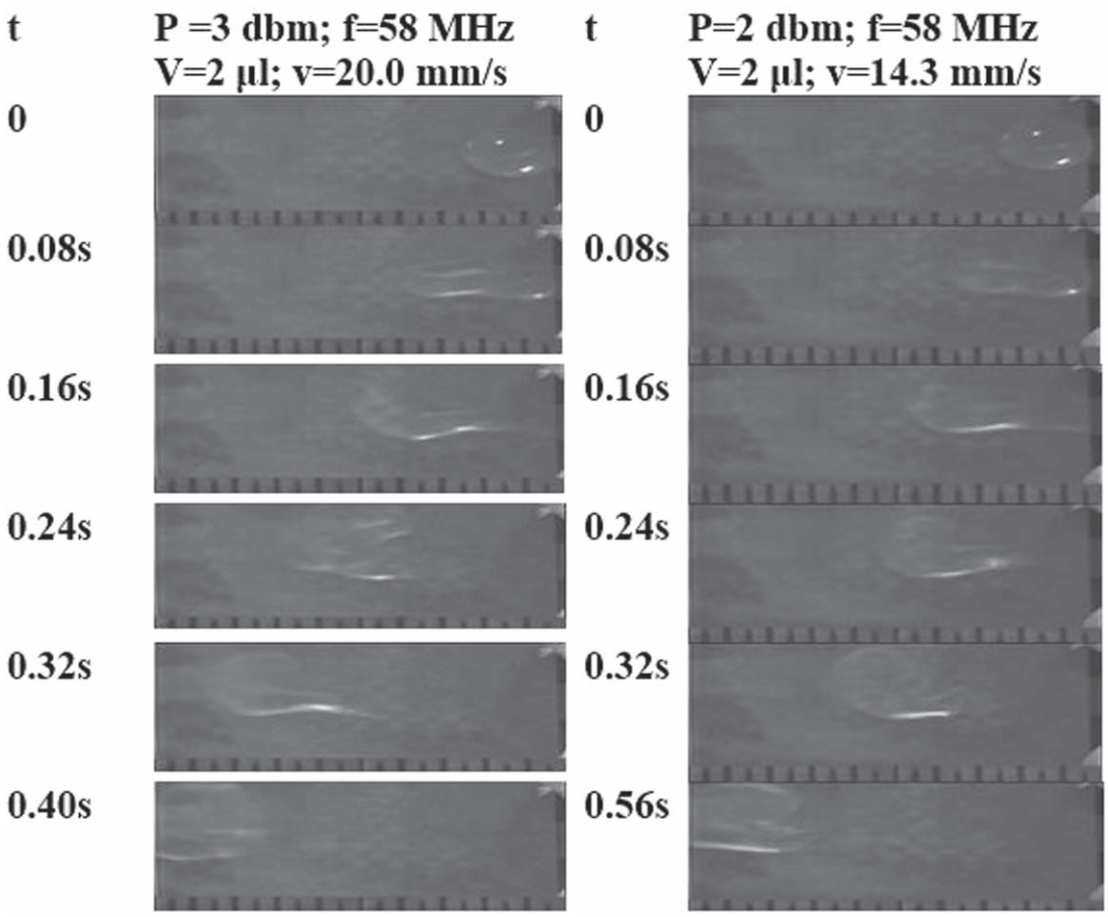

Figure 3. (Continued.)

used to apply a variable RF signal to IDTs using a time-dependent analysis. The bottom of the piezoelectric substrate was fixed and able to absorb vibrations, as well as not reflect the waves back.

First, we simulated the propagation of surface acoustic waves on a lithium niobate piezoelectric substrate, and then developed a new computing model that excite the fluid motion using the first part of simulation surface acoustic waves (SAW) on the surface of the piezoelectric crystal.

The substrate model uses a 128-degree *YX*-cut of lithium niobate substrate. IDT on this SAW device were modeled as ideal conductors using the boundary conditions (figure 1). IDT thickness is very small compared to the piezoelectric substrate, the influence of their mass and rigidity on the dynamics of the device were not taken into account.

SAW excited on the piezoelectric surface with the IDT at a certain resonant frequency. Figure 4 shows the geometry of the SAW device consisting of a lithium niobate ($LiNbO_3$) substrate and IDT electrodes and a liquid droplet placed on the surface of piezoelectric substrate (See figure 4). In this study, according to the problem statement, were measured and numerically calculated speed of the water droplet on the surface of a flat substrate.

The IDT has electrodes which are used to generate the SAW wavelength of $\lambda = 60\ \mu$m and sound velocity of 3488 m s^{-1}. We used the substrate thickness like a set to twice the wavelength for the computational efficiency. This is based on the assumption that SAW does not penetrate more into the depth of the substrate. To generate SAWs, a voltage with a 10 V high-frequency signal is applied to IDT. After applying SAW propagates along the surface of the substrate (see figure 1).

The piezoelectric effect connects mechanical and electrical components in the wave equation. From the basics of SAW, it is known that SAW propagation in a piezoelectric substrate is controlled through both stress and strain equation (electromechanical) of motion.

$$T = CE * S - eT * E \quad (1)$$

$$D = e * S + \varepsilon s * E \quad (2)$$

where T is the stress matrix; S—strain tensors; E is the electric potential field, D is the displacement vector. The parameters CE, εs, and e are the elasticity matrix, permittivity matrix and coupling matrix of the piezoelectric substrate respectively.

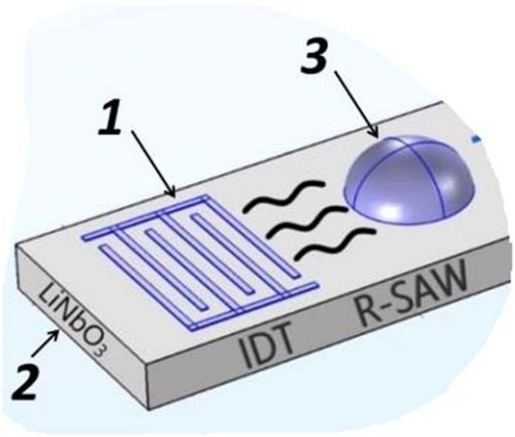

Figure 4. Figure illustrating the SAW device: 1—interdigital transducer (IDT); 2—piezoelectric substrate; 3—liquid droplet (a); Water penetration through the Nafion membranes were not shown.

Consider the wave equation taking into account the piezoelectric effect. The piezoelectric effect connects mechanical and electrical components in the wave equation.

$$\rho\frac{\partial u^2}{\partial t^2} - \nabla \cdot \sigma = F_v \tag{3}$$

where ρ is the density of the medium, u is the displacement field, σ is the voltage.

The Electrostatic equations are given in equation (4). Under static conditions, the electric potential V is determined by the relations:

$$\begin{aligned} \nabla \cdot D &= \rho_v \\ E &= -\nabla V \\ D &= D_r + e(\varepsilon - \varepsilon_0) + \varepsilon_0 \nu_{ac} \varepsilon_{rs} E \\ \varepsilon &= \frac{1}{2}(\nabla u + (\nabla u)^T) \end{aligned} \tag{4}$$

where ∇u—is the structure velocity field, ε_{rs}—relative permittivity, S—deformation, E—electric field, and D_r—electric displacement.

In this paper a three-dimensional (3D) mathematical model of the water droplet motion coupled with CWE was developed. To describe the motion of the fluid flow, we used a Laminar Two-Phase Flow, Moving Mesh interface (TPFMM) in COMSOL Multiphysics 5.2 version with a time-dependent study which solves the Navier–Stokes equation (5) for incompressible fluid flow:

$$\rho\frac{\partial u}{\partial t} + \rho(u \cdot \nabla)u = \nabla \cdot [-pI + \mu(\nabla u + (\nabla u)^T)] + F \tag{5}$$

$$\frac{\partial \rho}{\partial t} + \nabla \cdot (\rho u) = 0 \tag{6}$$

where ρ—the density (SI unit: kg m^{-3}); u—the velocity vector (SI unit: m s^{-1}); p—pressure (SI unit: Pa); F—the volume force vector (SI unit: N m^{-3}); I—Identity matrix; μ—dynamic viscosity (SI unit: Pa^*s).

Equation (5) is the momentum equation and (6) is the continuity equation. Here u denotes the mesh velocity and arises from the definition of time derivatives in the coordinate system of the deformed mesh. Poisson's equation is solved for mesh displacement.

The internal water flow visualisation modeled for water droplet (5 *μl*) in normal conditions by using the FEM approach in the three-dimension space which combined with the Moving Mesh interface. The Navier Slip boundary condition used for the free surface of the fluid drop and contact forces, also gravity force taken into account. The mesh Model Builder with Swept Distribution calibrated to Fluid dynamics. Analytical theory of thickness acoustic resonances in liquid droplet on solid substrate and the wave refraction problems developed in [25, 26]. The volume force vector components approach for describing oscillations induced by ultrasonic surface acoustic waves investigated in [27]. The volume force vector components obtained according to Shiokawa *et al* [14], Alghane *et al* [9], and Du *et al* [15].

$$\begin{aligned} Fx &= \rho(1 + \alpha_i^2)A^2\omega^2 k_i \cdot \exp(2(k_i x + \alpha_i k_i z)) \\ Fz &= \rho(1 + \alpha_i^2)A^2\omega^2 \alpha_i k_i \cdot \exp(2(k_i x + \alpha_i k_i z)) \end{aligned} \tag{7}$$

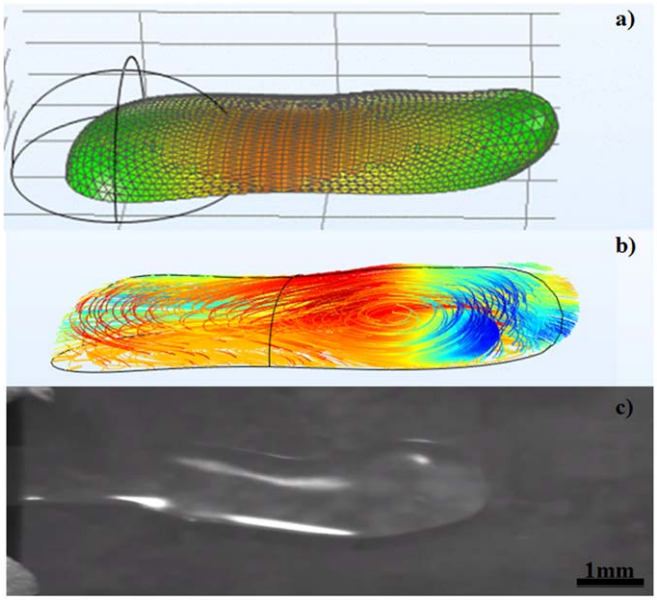

Figure 5. The simulation results (a)—moving mesh, (b)—streamlines) of water droplet motion under the influence of SAW compared with (c) experimental observation.

where $\alpha_i = j\alpha$, $k_L = k_r + jk_i$. F_x and F_z are the x and z components of the volume force F, respectively. Total SAW streaming force $F^2 = F_x^2 + F_z^2$. Coefficient A is the SAW amplitude which can be described using an expression (8) [8], in which P is the RF power applied to the SAW device in Watts.

$$A = \lambda^*8.15^*10^{-6}P^{0.225} + 5^*10^{-6}P^{0.8} \quad (8)$$

On the solid-fluid interface, the boundary conditions for the emission of plane waves into the second medium are established. SAW propagating across the substrate falls under the droplet. The model shown that due to the difference in the elastic wave propagation velocities under Rayleigh angle of acoustic radiation of the energy is transferred by acoustic radiation into the liquid, so-called leaky waves [8, 14]. Further, the obtained solution is used in the next modeling stage - the convection wave equation (CWE) which is necessary for modeling the propagation of ultrasound by the CWE module in water. The process of excitation of ultrasound in a liquid depends on an external source; therefore, for the CWE module, stitching conditions are set at the boundary. This analysis is needed to determine the local values of acceleration, velocity, and acoustic pressure in water. These data were useful for calculating the components of the total volume force, which acts on the droplet and falls in an exponential relationship as the acoustic radiation inside the water droplet. Further, using the laminar flow module in conjunction with a moving-variable grid, the components of the volume force acting on the water droplet were applied.

Corresponding parameters of dynamic viscosity, contact angle, and surface tension force were set. The simulation results show that the water droplet motion under the influence of SAW is consistent with the experimental observations in figure 5.

The simulation is achieved about 40 min. As a result, it is clear that, despite the physics of laminar flow, turbulence is used and internal streaming is observed (see figure 6). This is because the volume force is non-uniform and varies in-depth and in height of the drop as it moves away from the source of the surface acoustic wave.

4. Summary

The numerical modelling of the water droplet motion under the influence of SAW was carried out (see also [28]). A three-dimensional (3D) FEM for laminar TPFMM mathematical model coupled with CWE for the water droplet motion exited by SAW developed using COMSOL Multiphysics software. Water motions such as streaming, and droplet formation has been obtained numerically, and the simulation shape of droplet looked the same as in experimental observation. The simulation results of the water droplets give a value of 2.23 cm s^{-1}, which is in good agreement with the experiment (2.4 cm s^{-1}). These simulation results are important for clarifying the mechanism of interaction of SAW with a water droplet and for design laboratory devices on chips. Simulation can be used to calculate the shape of the droplet in dynamics, also, it is possible to predetermine the dependence of the curve of spreading the water volume with the speed of the droplet, depending on the power and frequency of the SAW numerically.

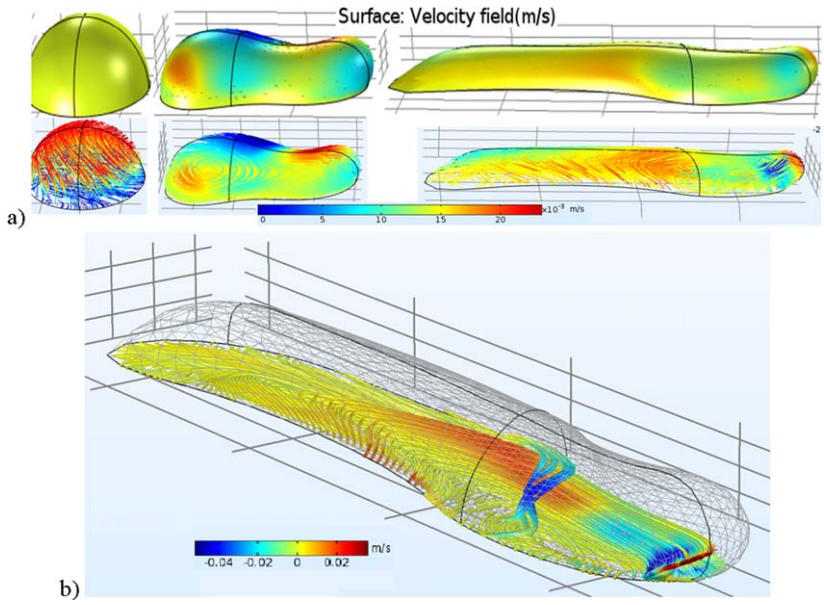

Figure 6 . (a) 3D Numerical model of a water droplet and its internal streaming flows. (b) Internal mixing visualization.

Acknowledgments

This work in part by the Nazarbayev University World Science Stars program, under Grant No. 031-2013 of 12/3/2013. One of the co-authors (N.Zh.) acknowledges a partial funding from Collaborative Research Project (CRP): 'Development of smart passive-active multiscale composite structure for earth Remote Sensing Satellites (RSS) of ultrahigh resolution (ULTRASAT)', Grant Award Nr. 091019CRP2115.). The authors are thankful to Jim Norem for proofreading the article.

Data availability statement

The data that support the findings of this study are available upon reasonable request from the authors.

Appendix

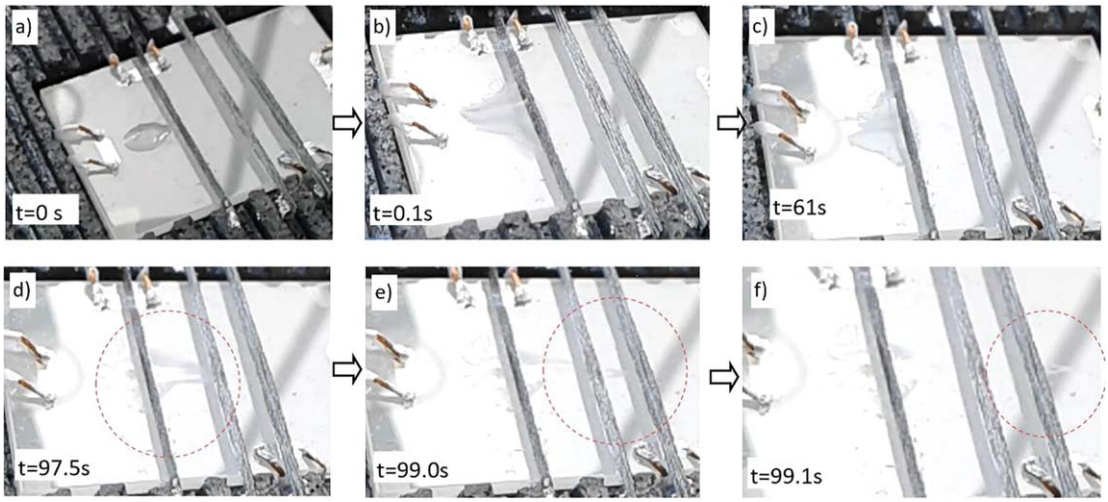

Figure A.1. Sequential side view images of the 2 μl droplet filtration dynamics under the influence of SAW through three Nafion membranes, each image has time indicators. Location of the transducer seen in the left side. (letters flow from left to right).

ORCID iDs

Zinetula Insepov https://orcid.org/0000-0002-8079-6293
Zamart Ramazanova https://orcid.org/0000-0002-2623-8901
Nurkhat Zhakiyev https://orcid.org/0000-0002-4904-2047

References

[1] Insepov Z, Wolf D and Hassanein A 2006 *Nano Lett.* **6** 1893–5
[2] Guttenberg Z V *et al* 2004 Flow profiling of a surface-acoustic-wave nanopump *Phys. Rev. E* **70** 056311
[3] Yeo L Y and Friend J R 2014 *Annu. Rev. Fluid Mech.* **46** 379–406
[4] Tan M K, Friend J R, Matar O K and Yeo L Y 2010 Capillary wave motion excited by high frequency surface acoustic waves *Phys. Fluids* **22** 112112
[5] Altshuler G and Manor O 2016 Free films of a partially wetting liquid under the influence of a propagating MHz surface acoustic wave *Phys. Fluids* **28** 072102
[6] Fu C, Quan A J, Luo J T *et al* 2017 *Appl. Phys. Lett.* **110** 173501
[7] Fu Y Q, Luo J K, Nguyen N T *et al* 2017 *Prog. Mater Sci.* **89** 31–91
[8] Guo Y J, Lv H B, Li Y F *et al* 2014 *J. Appl. Phys.* **116** 024501
[9] Alghane M, Fu Y Q, Chen B X *et al* 2011 *J. Appl. Phys.* **109** 114901
[10] Alghane M, Fu Y Q, Chen B X *et al* 2012 *J. Appl. Phys.* **112** 084902
[11] Alvarez M, Friend J and Yeo L Y 2008 *Nanotechnology* **19** 455103
[12] Kurosawa M, Watanabe T, Futami A *et al* 1995 *Sens. Actuators* **A50** 69–74
[13] Kurosawa M, Futami A and Higuchi T 1997 *Transducers* **97** 801–4
[14] Shiokawa S, Matsiu Y and Ueda T 1989 *IEEE 0090-5607/89/0000-0643 Ultrasonics symposium* 643–6
[15] Fu Y Q *et al* 2007 SAW streaming in ZnO surface acoustic wave micromixer and micropump,' SENSORS, 2007 IEEE *Atlanta, GA* 478–83
[16] Du X Y, Swanwick M E, Fu Y Q *et al* 2009 *J. Micromech. Microeng.* **19** 035016
[17] Karapetsas G, Chamakos N T and Papathanasiou A G 2016 *J. Phys.: Condens. Matter* **28** 085101 19
[18] Gorb A M, Nadtochii A B and Korotchenkov O A 2003 *J. Phys. Condens. Matter* **15** 7201–11
[19] Noori S S, Rahni M T and Taleghani S S 2020 Numerical analysis of droplet motion over a flat plate due to surface acoustic waves *Microgravity Sci. Technol.* **32** 647–60
[20] Comsol Multiphysics (https://comsol.com/comsol-multiphysics)
[21] Liang W and Lindner G 2013 Investigations of droplet movement excited by Lamb waves on a non-piezoelectric substrate *J. Appl. Phys.* **114** 044501
[22] Biroun M H, Rahmati M T, Jangi M, Tao R, Chen B X and Fu Y Q 2019 Computational and experimental analysis of droplet transportation/jetting behaviours driven by thin film surface acoustic waves *Sens. Actuators, A* **299** 111624
[23] Skov N R and Bruus H 2016 Modeling of microdevices for SAW-based acoustophoresis—a study of boundary conditions *Micromachines* **7** 182
[24] Phan H V, Alan T and Neild A 2016 Droplet manipulation using acoustic streaming induced by a vibrating membrane *Anal. Chem.* **88** 5696–703
[25] Begar A V, Nedospasov I A and Mozhaev V G 2014 Analytical theory of thickness acoustic resonances in liquid drop on solid substrate *2014 IEEE International Ultrasonics Symposium* 2012–4
[26] Tleukenov S K, Zhakiyev N K and Yeltinova L A 2013 An analytical solution of the reflection and refraction problems for coupled waves in elastic and piezoelectric media *2013 IEEE Int. Ultrasonics Symp. (IUS)* 1025–8
[27] Brunet P *et al* 2010 Droplet displacements and oscillations induced by ultrasonic surface acoustic waves: a quantitative study *Phys. Rev. E* **81.3** 036315
[28] Zhakiyev N, Tynyshtykbayev K and Insepov Z 2020 December Modeling and comparison with experiment of SAW induced water droplet motion *Journal of Physics: Conference Series* Vol **1696** 012036 IOP Publishing